Resolution beyond classical limits with spatial frequency heterodyning

A. Mudassar, A. R. Harvey, A. H. Greenaway, and J. D. C. Jones

School of Engineering and Physical Sciences, Heriot-Watt University, UK

Received October 19, 2005

A technique for coherent imaging based on spatial frequency heterodyning is described. Three images corresponding to three physical measurements are recorded. For the first measurement, a scene is simply illuminated with a coherent beam and for measurements 2 and 3, the scene is projected with cosine and sine fringes, respectively. Due to spatial frequency heterodyning, upper and lower side band information falls in the pass band of the imager. These bands are separated and correct phases and positions are assigned to these bands in the spatial frequency domain. An extension of bandwidth is achieved in the frequency domain and the inverse frequency domain data then give a high resolution coherent image.

OCIS codes: 100.6640, 170.3010, 110.1650.

A conventional imager acts as a low-pass filter to the spatial frequencies of a scene and consequently images recorded by such an imager have restricted resolution. Several techniques have been proposed[1−9] to enhance this resolution when the dimensions of the imager are fixed and the images are recorded under monochromatic illumination. Post-detection signal processing methods may be used to improve the spatial resolution, as determined by some heuristic resolution criterion (such as the Rayleigh criterion), by restoration of the pass-band filtered Fourier spectrum. These methods however enhance a discontinuity in the cutoff frequency in the spectra, resulting in strong Gibbs ringing in the restored image. Gibbs phenomena may be reduced by the use of a class of super-resolution algorithms that seek to infer the information beyond the cutoff frequency[1,2]. The performance of these algorithms depends on the signal-to-noise ratio of the images and on some a priori knowledge of the scene characteristics obtained using analytical or statistical methods[4,5] and the properties may vary from one scene to another. There are several techniques that help to encode the higher spatial frequency content of the scene onto lower frequency regions, so that all the spatial-frequency information can pass through the limited bandwidth of the imaging system. This concept was first used in the Lukosz techniques, reported by Lukosz[6], and Sun and Leith[7], which employ an interferometric mechanism consisting of multiple moving diffraction gratings. These gratings, when placed in front of the imaging lens, produce coupling between the spatial and temporal frequencies, so that higher spatial frequencies are shifted onto lower frequency bands that are transmitted by the optical system. These shifted bands have different temporal frequencies and may be restored by the use of a conjugate interferometric system positioned behind the lens.

In this paper a new scheme is proposed for extending the bandwidth of an imager based on spatial frequency heterodyning. In this technique, high spatial frequency cosine interference fringes illuminate the scene and heterodyne the scene spatial frequencies close to the fringe frequency to fall within the pass band of a conventional imager[9]. Three images are recorded: one with illumination of the scene with a coherent beam, second with illumination of the scene with cosine fringes and the third image recorded when the scene is illuminated with sine fringes. The use of a fringe frequency equal to twice the cutoff frequency of the imager increases the effective cutoff by a factor of three. Additional high-frequency components can be added by increasing the fringe frequency further to enable images of very high angular resolution to be constructed. The three images are used to separate out the low-pass-band, upper-side-band (USB) and lower-side-band (LSB). The USB and LSB are shifted to correct positions in the scene spectra by the convolution of these spectra with the frequency of the fringes.

Optical systems both coherent and incoherent are common in recording the intensity of a scene in which the phase information is lost. Due to very high temporal frequencies involved in optical domain, it is not possible to recover the phase information by generating a reference beam and then mixing it with the object beam as which is common in microwave imaging. Optical holography, however, provides a means of recording the amplitude as well as phase information of the field scattered off a scene as an object beam when a reference beam is mixed with the object beam at the imager usually consisting of an array of detectors. Optical holographic systems are restricted by the coherence length of the laser used in measurements when the path length differences involved are greater than the coherence length of the source. Distant imaging in optical domain using holography can be possible only if a reference beam is generated from spatially filtering a part of the scattered object field and then mixing it to the object beam. Imaging techniques that involve radio waves, microwaves and millimeter waves can employ holographic technique, as it is quite common and easier to generate a reference beam using highly stable local oscillators located at the imager side. This paper presents the mathematical modelling and simulation related to coherent optical systems which can be extended to three dimensional (3D) imaging by incorporating a reference beam at the imager.

A mathematical description of the process by which

scene is constructed is presented in following. Some examples illustrating the technique are also shown.

Mathematical modelling: following the scheme as presented by Mudassar *et al.*[9], three intensity measurements of a scene under the active coherent-illumination will be made. For measurement 1, the scene is simply illuminated with a coherent source for which the mathematical equation is given by Eq. (1). For measurements 2 and 3, the scene is illuminated with cosine and sine fringes. The measurements 2 and 3 can be described mathematically by Eqs. (2) and (3), respectively.

$$s_{\rm b}(x) = |u(x) \otimes h(x)|^2, \tag{1}$$

$$s_{\rm bc}(x) = |u(x)(1 + \cos(2\pi \cdot f \cdot x)) \otimes h(x)|^2, \tag{2}$$

$$s_{\rm bs}(x) = |u(x)(1 + \sin(2\pi \cdot f \cdot x)) \otimes h(x)|^2, \tag{3}$$

where $u(x)$ is the amplitude distribution at the scene; $h(x)$ is the amplitude point spread function of the optical coherent imager; $s_{\rm b}(x)$, $s_{\rm bc}(x)$ and $s_{\rm bs}(x)$ are the intensities measurements of the scene for the measurements 1, 2 and 3 respectively. The above equations are valid when the scene is located in the far field where the illuminating beams have plane incident waves. The equations below introduce some variables which will help to establish the application of the algorithm[9] to be applicable to the Eqs. (1)—(3),

$$u_{\rm b}(x) = u(x) \otimes h(x), \tag{4}$$

$$u_{\rm bc}(x) = u(x) \cdot \cos(2\pi \cdot f \cdot x) \otimes h(x), \tag{5}$$

$$u_{\rm bs}(x) = u(x) \cdot \sin(2\pi \cdot f \cdot x) \otimes h(x). \tag{6}$$

Equations (1)—(3) can be simplified as given below assuming that $u(x)$ is real

$$s_{\rm b}(x) = |u_{\rm b}(x)|^2 = I_{\rm b}(x), \tag{7}$$

$$\begin{aligned} s_{\rm bc}(x) &= |u_{\rm b}(x) + u_{\rm bc}(x)|^2 \\ &= I_{\rm b}(x) + I_{\rm bc}(x) + 2u_{\rm b}(x) \cdot u_{\rm bc}(x), \end{aligned} \tag{8}$$

$$\begin{aligned} s_{\rm bs}(x) &= |u_{\rm b}(x) + u_{\rm bs}(x)|^2 \\ &= I_{\rm b}(x) + I_{\rm bs}(x) + 2u_{\rm b}(x) \cdot u_{\rm bs}(x). \end{aligned} \tag{9}$$

If $\Im\{s_{\rm b}(x)\} = S_{\rm b}(k)$, $\Im\{s_{\rm bc}(x)\} = S_{\rm bc}(k)$ and $\Im\{s_{\rm bs}(x)\} = S_{\rm bs}(k)$ where $\Im$ is the Fourier transform (FT) operator then the Fourier transforms of the Eqs. (7)—(9) can be rearranged as

$$\begin{aligned} s_{\rm bc}(k) - s_{\rm b}(k) &= \Im\{I_{\rm bc}(x)\} + 2\Im\{u_{\rm b}(x)\} \otimes \Im\{u_{\rm bc}(x)\} \\ &= \Im\{u_{\rm bc}(x)\} \otimes \{\Im\{u_{\rm bc}(x)\} + 2\Im\{u_{\rm b}(x)\}\}, \end{aligned} \tag{10}$$

$$\begin{aligned} s_{\rm bs}(k) - s_{\rm b}(k) &= \Im\{I_{\rm bs}(x)\} + 2\Im\{u_{\rm b}(x)\} \otimes \Im\{u_{\rm bs}(x)\} \\ &= \Im\{u_{\rm bs}(x)\} \otimes \{\Im\{u_{\rm bs}(x)\} + 2\Im\{u_{\rm b}(x)\}\}. \end{aligned} \tag{11}$$

The USB can now be found as

$$\begin{aligned} \text{USB} &= (s_{\rm bc}(k) - s_{\rm b}(k)) - i(s_{\rm bs}(k) - s_{\rm b}(k)) \\ &= (\Im\{u_{\rm bc}(x)\} \otimes \Im\{u_{\rm bc}(x)\}) \\ &\quad -i(\Im\{u_{\rm bs}(x)\} \otimes \Im\{u_{\rm bs}(x)\}) \\ &\quad +(\Im\{u_{\rm bc}(x)\} - i\Im\{u_{\rm bs}(x)\}) \otimes 2\Im\{u_{\rm b}(x)\} \\ &= (1+i)\left(\frac{1}{4}g(k+f)H(k) \otimes g(k+f)H(k)\right. \\ &\quad \left. +\frac{1}{4}g(k-f)H(k) \otimes g(k-f)H(k)\right) \\ &\quad +(1-i)\frac{1}{2}g(k+f)H(k) \otimes g(k-f)H(k) \\ &\quad +2g(k+f)H(k) \otimes \Im\{u_{\rm b}(x)\}, \end{aligned} \tag{12}$$

where $\Im\{u(x)\} = g(k)$. It has been assumed that $u(x)$ is real and positive. Under such a condition the magnitude of the 0th order frequency (with no complex part) in $\Im\{u_{\rm b}(x)\}$ is very much dominant over the magnitudes of the remainder of the spectral frequencies in the pass-band of the imager. The convolution of $g(k+f)$ would be quite dominant as comparing with its convolution with other frequencies. It would be appropriate to write

$$2g(k+f)H(k) \otimes \Im\{u_{\rm b}(k)\} \approx \alpha \cdot g(k+f) \cdot H(k), \tag{13}$$

where α is equal to twice the magnitude of the 0th order frequency in $\Im\{u_{\rm b}(x)\}$. Moreover, the term in Eq. (13) is much larger as compared with the remainder of the terms in Eq. (12), which can be written as

$$\text{USB} \approx \alpha \cdot g(k+f) \cdot H(k). \tag{14}$$

Similarly, the LSB can be written as

$$\begin{aligned} \text{LSB} &= (s_{\rm bc}(k) - s_{\rm b}(k)) + i(s_{\rm bs}(k) - s_{\rm b}(k)) \\ &\approx \alpha \cdot g(k-f) \cdot H(k). \end{aligned} \tag{15}$$

The right hand sides of Eqs. (14) and (15) can now be de-convolved as usual to find the desired terms for extended spectrum and de-convolutions are given below

$$\begin{aligned} &g(k+f)H(k) \otimes \left(\frac{1}{2}\delta(k+f) + \frac{1}{2}\delta(k-f)\right) \\ &= \frac{1}{2}g(k+2f)H(k+f) + \frac{1}{2}g(k)H(k-f), \end{aligned} \tag{16}$$

$$\begin{aligned} &g(k-f)H(k) \otimes \left(\frac{1}{2}\delta(k+f) + \frac{1}{2}\delta(k-f)\right) \\ &= \frac{1}{2}g(k)H(k+f) + \frac{1}{2}g(k-2f)H(k-f). \end{aligned} \tag{17}$$

The extended spectrum $g_{\rm E}(k)$ is given by combining the second term on the right hand side of Eq. (16), the

first term on the right hand side of Eq. (17) along with the spectrum corresponding to Eq. (4) and is given as

$$g_{\mathrm{E}}(k) = g(k)(H(k+f) + H(k) + H(k-f))$$
$$= g(k) \cdot H_{\mathrm{E}}(k). \tag{18}$$

The inverse Fourier transform of both sides of Eq. (18) gives the synthesised amplitude of the scene as

$$u_{\mathrm{E}}(x) = u(x) \otimes h_{\mathrm{e}}(x). \tag{19}$$

Comparing Eq. (19) with Eq. (1), it is revealed that the synthesized image is a high resolution image and in this particular case the synthesis is three times the band-limited image given by Eq. (1).

Computer simulation: to elaborate the concept of spatial frequency heterodyning, a simple image consisting of straight lines of varying spatial frequency was chosen as shown in Fig. 1(a). Three images were obtained from the image shown in Fig. 1(a) according to Eqs. (1)—(3) and are shown in Figs. 1(b), (c) and (d) respectively. The explicit form of the point spread function used in the simulation is $h(x) = \sin(\pi x)/\pi x$. The image in Fig. 1(b) is a band-limited version of the image shown in Fig. 1(a). The images in Figs. 1(c) and (d) were obtained when the image in Fig. 1(a) was projected with cosine and sine fringes, respectively. The three images were then processed according to the mathematical modelling and a high resolution image was obtained according to Eq. (19), as shown in Fig. 1(e). The concept of spatial frequency heterodyning is quite obvious from the images in Figs. 1(c) and (d). In the simulation, the spatial frequency of the fringes was twice the spatial cutoff frequency of the imager.

In the simulation shown in Fig. 1, one-dimensional (1D) image was considered and one orientation of fringes was used to elaborate and to synthesize the high-resolution image. For two-dimensional (2D) images, four orientations of fringes are required to synthesize the images in four orientations at 0°, 45°, 90°, and 135° and the final image is given by combining the individually obtained synthesized images. The image in Fig. 2(a) was taken as original image for simulation. The image in Fig. 2(b) is a band-limited image obtained from Fig. 2(a) using Eq. (1) with appropriate point spread function. The images shown in Figs. 2(c) and (d) correspond to cosine and sine fringes with 0° orientation. Three pairs of images similar to the ones shown in Figs. 2(c) and (d) were obtained for orientation of fringes at 45°, 90° and 135°. Four synthesized images were obtained corresponding to four orientations of fringes and were combined to form the final synthesized image shown in Fig. 2(e). The original scene in Fig. 2(a) was assumed to be optically flat to get rid of speckles.

The image shown in Fig. 2(a) was optically flat and this was made optically rough by multiplying it with a complex phase screen as shown in Fig. 3(a). The optically rough image was imaged with a band-limited imager and the image obtained is shown in Fig. 3(b). The images in Figs. 3(c) and (d) were obtained with cosine and sine fringes when projected on the rough scene with 0° orientation. Three pairs of images (not shown) were also obtained for other orientations of the fringes. The final

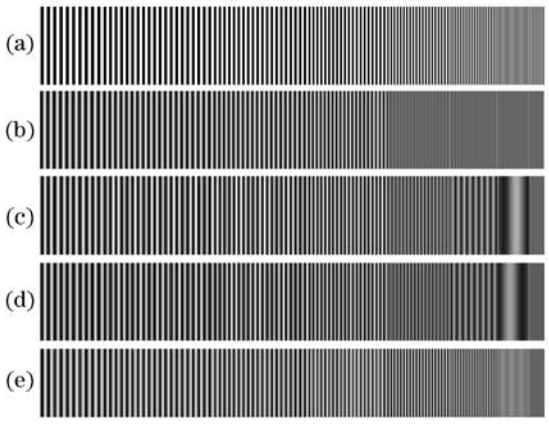

Fig. 1. Computer simulated result showing spatial frequency heterodyning concept. (a) Original image; (b) image obtained with a low pass imager; (c) image obtained when scene in (a) was projected with cosine fringes; (d) image obtained when scene in (a) was projected with sine fringes; (e) reconstructed super resolution image.

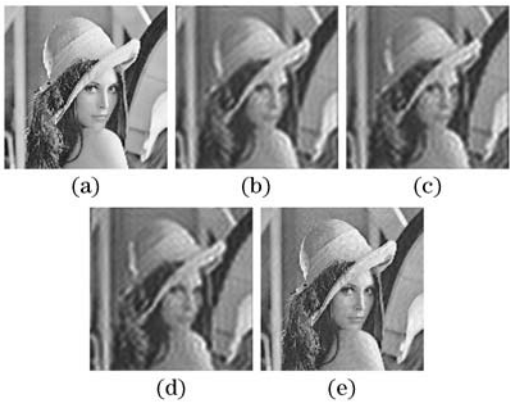

Fig. 2. Simulation results for coherently obtained optically plane imagess. (a) Original image; (b) band-limited image; (c) image corresponding to measurement 2 for vertical orientation of fringes; (d) image corresponding to measurement 3 with vertical orientation of fringes; (e) overall synthesized image.

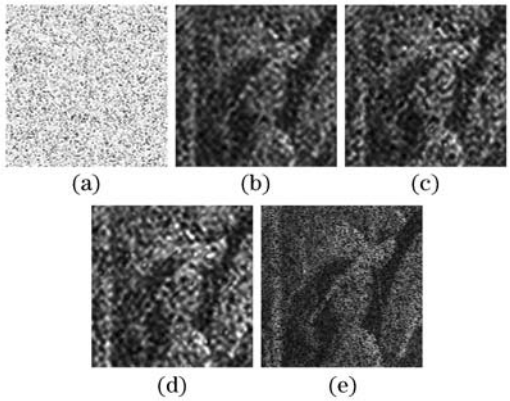

Fig. 3. Simulation results for coherently obtained optically rough images. (a) Complex phase screen used to make image in Fig. 2(a) an optically rough scene; (b) band-limited image; (c) image corresponding to measurement 2 for vertical orientation of fringes; (d) image corresponding to measurement 3 with vertical orientation of fringes; (e) overall synthesized image.

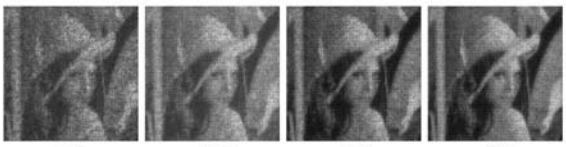

Fig. 4. Simulation results for coherently obtained optically rough images added incoherently with varying phase screen distribution. (a) Incoherent addition of 10 synthesized images; (b) incoherent addition of 20 synthesized images; (c) incoherent addition of 40 synthesized images; (d) incoherent addition of 60 synthesized images.

synthesized image is shown in Fig. 3(e). The presence of speckles in all the images has spoiled the resolution, which is otherwise obvious in the corresponding images of Fig. 2.

The effect of speckles can be minimized using many techniques[9]. One technique is to incoherently add the synthesized images. When 10 synthesized images like the one shown in Fig. 3(e) were incoherently added, the resultant image is shown in Fig. 4(a). The resultant images with incoherent addition of synthesized images with 20, 40 and 60 images are respectively shown in Figs. 3(b), (c), and (d). A few images are required in the incoherent addition to obtain a speckle free image if the images have uncorrelated speckles.

In conclusion, a super-resolution technique for coherent imaging systems has been described by using spatial frequency heterodyning. Three snapshots of a scene are recorded and through simple mathematical algorithm, a high resolution image is obtained. The spatial frequency of the projected fringes was twice the spatial cutoff frequency of the imager. The images have been simulated for three-times high resolution. In principle, it is possible to extend the resolution beyond three times the resolution without aperture synthesis by repeating the process with increased spatial frequency of the fringes. The effect of speckles on the synthesized images has been simulated and incoherent averaging of synthesized images has shown reduction in speckles in the final image. The phase of the projected fringes must be known accurately in order to assign correct phases to the upper and lower side bands in the reconstructed spectrum.

A. Mudassar's e-mail address is asloob@yahoo.com.

References

1. J. L. Harris, J. Opt. Soc. Am. **54,** 931 (1964).
2. R. W. Gerchberg, Opt. Acta **21,** 709 (1974).
3. P. J. Sementilli, B. R. Hunt, and M. S. Nadar, J. Opt. Soc. Am. A **10,** 2265 (1993).
4. M. Fuderer, Proc. SPIE **1137,** 84 (1989).
5. A. H. Lettington and Q. H. Hong, IEE Proc. **141,** 9 (1994).
6. W. Lukosz, J. Opt. Soc. Am. **57,** 932 (1967).
7. P. C. Sun and E. N. Leith, Appl. Opt. **31,** 4857 (1992).
8. A. H. Letting, Q. H. Hong, and S. Tzimopoulou, Appl. Opt. **35,** 5258 (1996).
9. A. Mudassar, A. R. Harvey, A. H. Greenaway, and J. Jones, J. Phys.: Conf. Ser. **15,** 290 (2005).